ISBN: 978-3-95450-261-5 ISSN: 2673-7000 doi: 10.18429/JACoW-NAPAC2025-MOP015

BEAM SCATTERING THROUGH FOIL*

B. Dhital†, P. Adams, K.A. Brown, T. Olsen, N. Tsoupas, W. Lin
Brookhaven National Laboratory, NY, USA
D. Sagan, Cornell University, NY, USA

Abstract

This paper describes the foil structure used at the beam extraction point in the NASA Space Radiation Laboratory (NSRL) beamline. The stripping foil removes electrons from incoming ions, rendering them partially or fully stripped. Foils of various materials and thicknesses are employed, enabling ion species at different energies to pass through. As charged particles traverse a foil, the outgoing particles exhibit a Gaussian-like angular distribution. This distribution is subsequently transformed into a uniform profile by a set of octupole magnets, essential for various beam experiments at the NSRL target. We utilize the Bmad and SRIM computer codes to calculate the energy loss through the foils for different ion species, energies, and charge states. After preparing ion beam species in the Booster, we determine the energy loss by measuring the horizontal beam profile at the multi-wire MW063 location in the NSRL beamline. Finally, we present a summary of energy loss calculations obtained through Bmad, SRIM, and experimental data.

INTRODUCTION

When charged particles pass through a thin, material medium, they receive a random directional "kick", altering their angle of motion. This interaction collectively shapes the resulting phase space into a more Gaussian-like angular distribution [1]. In addition to this angular modification, particles also lose energy and may undergo charge-changing interactions as they pass through the material. These effects are crucial for shaping the ion species beam used at the NASA Space Radiation Laboratory (NSRL). These experiments require a large uniform beam area which is achieved through two octupole magnets in opposing polarity [2, 3] which would not be possible with the distorted, one-third integer resonant slow extracted phase space produced by such an extraction scheme [4–6].

The multiple scattering process through a foil is dominated by a screened Coulomb interaction between the projectiles (protons and ions) and target atom. A foil element in general, represents a planar sheet of material which strips electrons from an incoming particle towards it. In conjunction, there will be scattering of the particle trajectory as well as an associated energy loss [7]. In this paper, we measure the multiple scattering of primary beam ions incident upon the copper foils at NSRL beamline and compare the measurement with the results calculated from Bmad [7] and the SRIM code [8, 9].

* Work supported by Brookhaven Science Associates, LLC, under Contract No. DE-AC02-98CH10886 with the U.S. Department of Energy and by NASA (Contract No. T570X), and by NSF under Award PHY-1549132.
† bdhital@bnl.gov

ACCELERATOR & BEAMLINE OVERVIEW

The Booster is a 201.78 m circumference separated-function synchrotron that accelerates protons and heavy ions from EBIS, Tandem, and LINAC injectors using one-third integer resonant slow extraction [3, 5], with ions heavier than protons accelerated in intermediate charge states [10] (Fig. 1). Ions are extracted from the Booster using the one-third integer resonant slow extraction method [5].

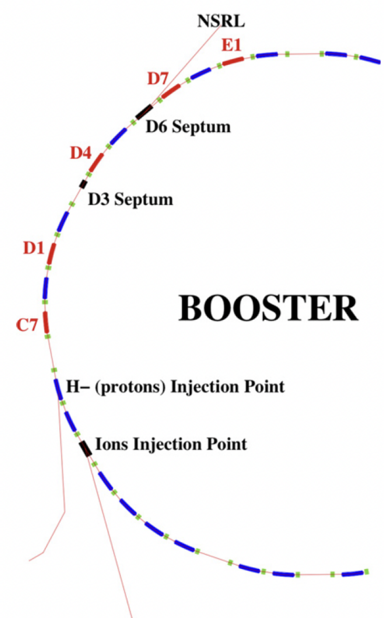

Figure 1: Layout of the portion of the Booster ring showing five extraction bumps (C7, D1, D4, D7, and E1) and two extraction septa magnets (D3 and D6) to enhance slow resonant extraction of beam to the NSRL beamline.

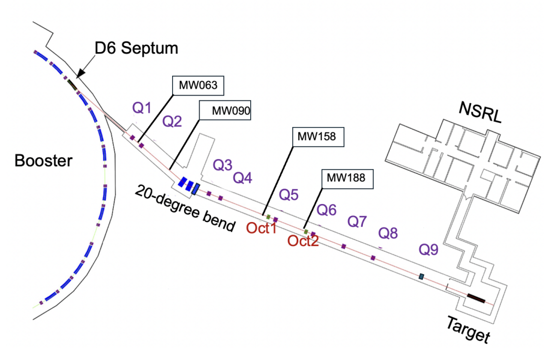

Figure 2: Layout of the NSRL beam line starting at D6 septum magnet where slow extracted beam from the Booster passes through the foil element.

ISBN: 978-3-95450-261-5 ISSN: 2673-7000 doi: 10.18429/JACoW-NAPAC2025-MOP015

A schematic layout of the NSRL beam line is shown in Fig. 2. The approximate 100 m line consists of a dipole triplet (labeled 20-degree bend), nine quadrupole magnets Q1-Q9, two octupoles, and several corrector dipoles. The two octupoles, can be adjusted to achieve a uniform rectangular distribution of beam on target. The beam optics of the line are designed to produce an achromatic beam after the 20° dipole triplet magnets. This is important for achieving the necessary large and uniform beams. Momentum-dependent motion at the entrance to the octupoles will affect uniformity. Table 1 shows the states of some of the ions before and after they are stripped of electrons respectively.

Table 1: Ion species with initial and final charge states used in our study at the NSRL.

Ion Species	$Q_{\mathrm{foil,in}}$	$Q_{\mathrm{foil,out}}$	**Mass No. (A)**
Si	+11	+14	28
Fe	+20	+26	56
Tb	+35	+65	159

FOIL SCATTERING

The scattering angle (σ_{scatt}) is defined following Lynch and Dahl [11–13] as

$$\sigma_{\mathrm{scatt}} = \frac{S_z z}{p\beta}\sqrt{\frac{X}{X_0}}\left[1 + \varepsilon\, log_{10}\left(\frac{Xz^2}{X_0\beta^2}\right)\right], \tag{1}$$

where p, β, and z are the momentum, speed, and charge number of the incident particle, and X/X_0 is the thickness of the scattering medium in radiation length. The parameters S_z abd ε and their values are explained in details in the reference [11].

Energy Loss Through Foil

For a particle with speed v, charge z, and energy E, traveling a distance x into a foil target of electron number density n and mean excitation energy I, the relativistic formula to calculate the energy loss is given by [14]

$$-\left\langle\frac{dE}{dx}\right\rangle = \frac{4\pi nz^2}{m_e c^2\beta^2}\left(\frac{e^2}{4\pi\varepsilon_0}\right)^2\left[\log_{10}\left(\frac{2m_e c^2\beta^2}{I(1-\beta^2)}\right) - \beta^2\right], \tag{2}$$

where c is the speed of light, ε_0 is the vacuum permittivity, $\beta = v/c$ is the relativistic velocity, e, and m_e are electronic charge and rest mass of electron respectively. The electron density n of the material can be calculated by using the following formula

$$n = \frac{N_A.Z.\rho}{A.M_u}, \tag{3}$$

where N_A is the Avogadro number, Z its atomic number, ρ is the density of the material, A is its relative atomic mass, and M_u is the molar mass constant. The total energy loss through foil ΔE is then calculated multiplying $-\left\langle\frac{dE}{dx}\right\rangle$ by dx, the total foil thickness.

Energy Loss Calculations

Ion beams (Si, Fe, Tb) at different energies pass through copper foils of varying thickness to measure energy loss. The horizontal beam profile at multi-wire MW063 is analyzed, with all quadrupoles between D6 septum magnet and MW063 turned off. The D6 septum magnet bends the beam by a constant angle 155 m-rad. We start from minimum thickness foil and increase thickness for each case. For the D6 septum magnet with length L, we assume BL is constant:

$$\theta = \frac{BL}{B\rho}, \tag{4}$$

where $B\rho$ is the beam rigidity. Initially with no foil, θ_0 is the bend angle for rigidity $(B\rho)_0$ and measured beam position is x_0. After introducing foil, the beam is fully stripped with energy loss. The new beam position x_1 at MW063 gives new rigidity $(B\rho)_1$ and bend angle:

$$\theta_1 = \theta_0 + \frac{(x_1 - x_0)}{S}, \tag{5}$$

where S is the distance between D6 and MW063. Beam rigidity is defined by:

$$B\rho = k\,\frac{p(GeV/c)}{q}, \tag{6}$$

where $k = 10^9/3 \times 10^8$. Then $(pc)_1$ is calculated as:

$$(pc)_1 = \frac{(B\rho)_1}{k}q \tag{7}$$

Since BL is constant, $(B\rho)_1 = \theta_0(B\rho)_0/\theta_1$. Using the relativistic formula, total energy is:

$$E_{T_1}^2 = E_0^2 + (pc)_1^2, \tag{8}$$

where E_0 is the ion rest mass energy. Kinetic energy is:

$$E_k = E_{T_1} - E_0. \tag{9}$$

We calculate kinetic energy per nucleon (MeV/n) before and after the foil to determine energy loss. The schematic diagram to run this measurement is shown in Fig. 3.

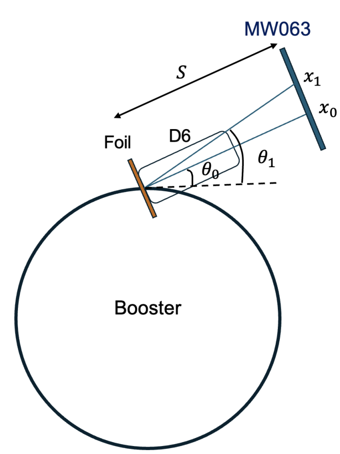

Figure 3: Beam centroid positions at MW063 before (x_0) and after (x_1) foil insertion for varying copper foil thicknesses.

ISBN: 978-3-95450-261-5 ISSN: 2673-7000 doi: 10.18429/JACoW-NAPAC2025-MOP015

Table 2 presents energy loss calculations for Si, Fe, and Tb using three methods across various copper foil thicknesses. The corresponding data are plotted in Fig. 4, Fig. 5, and Fig. 6 respectively.

Table 2: Energy Loss Calculations for Various Ion Species and Foil Thickness (thk)

Ion	thk	Energy Loss (MeV/n)		
	(mm)	Bmad	SRIM	Measurement
Si	0.025	−0.27	−0.27	−0.27 ± 0.033
618	0.127	−1.39	−1.36	−1.36 ± 0.037
MeV/n	0.254	−2.78	−2.72	−2.73 ± 0.047
	0.381	−4.17	−4.07	−4.08 ± 0.067
Fe	0.025	−0.52	−0.50	−0.49 ± 0.029
493	0.127	−2.60	−2.48	−2.29 ± 0.155
MeV/n	0.254	−5.20	−5.04	−4.83 ± 0.189
	0.381	−7.81	−7.60	−7.10 ± 0.364
	0.508	−10.43	−10.17	−9.89 ± 0.270
	0.635	−13.05	−12.73	−12.23 ± 0.410
Tb	0.254	−12.55	−11.92	−11.92 ± 0.367
402	0.381	−18.89	−17.88	−17.55 ± 0.698
MeV/n	0.508	−25.27	−23.84	−23.55 ± 0.924
	0.635	−31.70	−29.96	−27.31 ± 2.207

Error bars represent combined uncertainties from beam position measurement precision and systematic errors, providing a comprehensive estimate of experimental measurement uncertainty.

SUMMARY

We analyzed energy loss calculations for Iron (493 MeV/u), Terbium (402 MeV/u), and Silicon (618 MeV/u) ions passing through copper foils using three methods: SRIM calculations, position-based measurements at MW063, and Bmad simulations. While Bmad predicted slightly higher energy losses (particularly for Terbium), all methods showed good agreement within acceptable limits for heavy ion physics, validating our energy loss measurements.

REFERENCES

[1] T. Yamazaki, M. Takasaki, and M. Sakisaka, "Multiple scattering of protons and nitrogen ions on metal foils", *Journal of the Physical Society of Japan*, vol. 36, no. 6, pp. 1643–1648, 1974. doi:10.1143/JPSJ.36.1643

[2] N. Tsoupas *et al.*, "Uniform beam distributions at the target of the NASA Space Radiation Laboratory's beam line", *Physical Review Special Topics-Accelerators and Beams*, vol. 10, no. 2, p. 024 701, 2007. doi:10.1103/PhysRevSTAB.10.024701

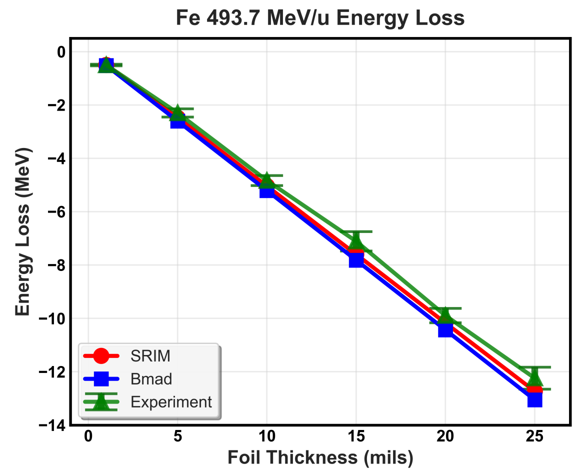

Figure 4: Energy loss calculation for Iron at 493.7 MeV/n through copper foils of varying thickness.

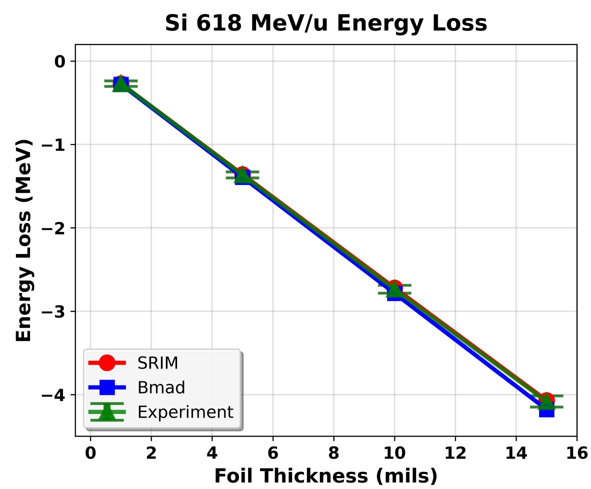

Figure 5: Energy loss calculation for Silicon at 618 MeV/n through copper foils of varying thickness.

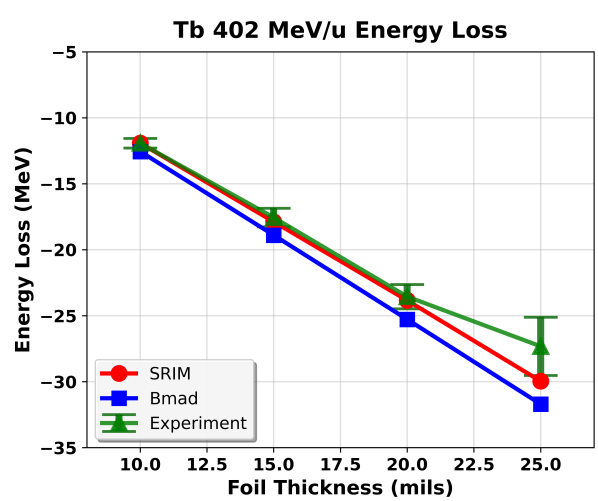

Figure 6: Energy loss calculation for Terbium at 402 MeV/n through copper foil of varying thickness.

ISBN: 978-3-95450-261-5 ISSN: 2673-7000 doi: 10.18429/JACoW-NAPAC2025-MOP015

[3] K. Brown *et al.*, "The NASA Space Radiation Laboratory at Brookhaven National Laboratory: Preparation and delivery of ion beams for space radiation research", *Nuclear Instruments and Methods in Physics Research Section A: Accelerators, Spectrometers, Detectors and Associated Equipment*, vol. 618, no. 1-3, pp. 97–107, 2010. doi:10.1016/j.nima.2010.02.276

[4] K. Brown *et al.*, "Design of a resonant extraction system for the ags booster", in *Proceedings of the 1999 Particle Accelerator Conference (Cat. No.99CH36366)*, p. 1270–1272 vol.2, 1999. doi:10.1109/PAC.1999.795518

[5] K. Brown *et al.*, "Resonant extraction parameters for the ags booster", in *PACS2001. Proceedings of the 2001 Particle Accelerator Conference (Cat. No.01CH37268)*, p. 1517–1519 vol.2, 2001. doi:10.1109/PAC.2001.986733

[6] N. Tsoupas *et al.*, "Results from the commissioning of the nsrl beam transfer line at bnl", in *Proceedings of the 2004 European Particle Accelerator Conference, Luzern*, pp. 2879–2881, 2004. https://accelconf.web.cern.ch/e04/PAPERS/THPLT183.PDF

[7] D. Sagan, "Bmad: A relativistic charged particle simulation library", *Nuclear Instruments and Methods in Physics Research Section A: Accelerators, Spectrometers, Detectors and Associated Equipment*, vol. 558, no. 1, pp. 356–359, 2006. doi:10.1016/j.nima.2005.11.001

[8] J. F. Ziegler and J. P. Biersack, "The stopping and range of ions in matter", in *Treatise on Heavy-Ion Science: Volume 6: Astrophysics, Chemistry, and Condensed Matter*, Springer, 1985, pp. 93–129. doi:10.1007/978-1-4615-8103-1_3

[9] J. F. Ziegler, M. D. Ziegler, and J. P. Biersack, "SRIM–the stopping and range of ions in matter (2010)", *Nuclear Instruments and Methods in Physics Research Section B: Beam Interactions with Materials and Atoms*, vol. 268, no. 11-12, pp. 1818–1823, 2010. doi:10.1016/j.nimb.2010.02.091

[10] T. Olsen and K. A. Brown, "High energy, heavy ion testing at Brookhaven National Laboratory", in *2024 IEEE Radiation Effects Data Workshop (REDW) (in conjunction with 2024 NSREC)*, pp. 1–6, 2024. doi:10.1109/redw61286.2024.10759172

[11] G. R. Lynch and O. I. Dahl, "Approximations to multiple coulomb scattering", *Nuclear Instruments and Methods in Physics Research Section B: Beam Interactions with Materials and Atoms*, vol. 58, no. 1, pp. 6–10, 1991. doi:10.1016/0168-583X(91)95671-Y

[12] H. A. Bethe, "Moliere's theory of multiple scattering", *Physical Review*, vol. 89, no. 6, p. 1256, 1953. doi:10.1103/PhysRev.89.1256

[13] C. Case and E. Battle, "Molière's theory of multiple scattering", *Physical Review*, vol. 169, no. 1, p. 201, 1968. doi:10.1103/PhysRev.169.201

[14] H. Bethe, "Zur theorie des durchgangs schneller korpuskularstrahlen durch materie", *Annalen der Physik*, vol. 397, no. 3, pp. 325–400, 1930. doi:10.1002/andp.19303970303